The electronic structure of 4d transition-metal monatomic wires

2004 J. Phys.: Condens. Matter 16 8061

(http://iopscience.iop.org/0953-8984/16/45/028)

INSTITUTE OF PHYSICS PUBLISHING JOURNAL OF PHYSICS: CONDENSED MATTER

J. Phys.: Condens. Matter **16** (2004) 8061–8074 PII: S0953-8984(04)82140-4

The electronic structure of 4d transition-metal monatomic wires

A Delin[1,2] **and E Tosatti**[2,3,4]

[1] Materialvetenskap, Brinellvägen 23, KTH, SE-10044 Stockholm, Sweden
[2] Abdus Salam International Center for Theoretical Physics (ICTP), Strada Costiera 11, 34100 Trieste, Italy
[3] International School for Advanced Studies (SISSA), via Beirut 2–4, 34014 Trieste, Italy
[4] INFM DEMOCRITOS National Simulation Center, via Beirut 2–4, 34014 Trieste, Italy

E-mail: anna.delin@mse.kth.se

Received 15 June 2004, in final form 4 October 2004
Published 29 October 2004
Online at stacks.iop.org/JPhysCM/16/8061
doi:10.1088/0953-8984/16/45/028

Abstract

Monatomic nanowires of the nonmagnetic transition metals Ru, Rh, and Pd have been studied theoretically, using first-principles computational techniques, in order to investigate the possible onset of magnetism in these nanosystems. Our fully relativistic spin-polarized all-electron density functional calculations reveal the onset of Hund's rule magnetism in nanowires of all three metals, with mean-field moments of 1.1, 0.3, and 0.7 μ_B, respectively, at the equilibrium bond length. An analysis of the band structures indicates that the nanocontact superparamagnetic state suggested by our calculations should affect the ballistic conductance between tips made of Ru, Rh or Pd, leading to possible temperature and magnetic field dependent conductance.

1. Introduction

Reducing the dimensionality and size of a metallic object eventually leads to quantum confinement of the electrons in one or more dimensions. Examples of such systems are metallic nanowires, where the electrons are confined in two dimensions, but unconfined in the third dimension, along the wire. The ultimately smallest metallic wire consists of just a single metallic chain of atoms. Experimentally, long segments of such nanowires have been realized, in particular of Au [1, 2]. The production of shorter segments was recently reported for several other metals including the 4d transition metals Ru, Rh [3], and Pd [4]. The quantum confinement of the electrons in the wires results in intriguing behaviour with respect to their mechanical, electrical and chemical properties and causes new physical phenomena to appear, for example quantized conductance [5] and helical geometries [6, 1, 7]. Thus, the properties of these nanosystems may be dramatically different from the bulk properties of the same metals.

In particular, it is interesting to explore whether and how nanowires of bulk nonmagnetic metals can become magnetic, and how other properties of these nanosystems in turn are affected by the presence of magnetism in the nanosystem, especially of a genuine Hund's rule magnetic order parameter.

We recently performed a similar study of the 5d metals Os, Ir, and Pt, which revealed intriguing magnetic properties of nanowire systems. In the present paper, we concentrate on the 4d transition metals Ru, Rh, and Pd, and contrast our results for these metals with our results for the corresponding 5d systems. We investigate the possibility of ferromagnetism[5] and its effect on other properties, notably quantized conductance for straight monostrand nanowires of these metals, using state-of-the-art all-electron computational methods based on density functional theory. We have also performed the corresponding calculations for the noble metal Ag, where no magnetism is expected, for comparison.

We address here the physics of metallic nanowires suspended between two leads, where transmission electron microscope images on monostrand nanowires indicate straight wire geometries [4]. Nanowires can be stabilized in this way only temporarily, as the flow of atoms to the leads inevitably implies stretching and thinning, which eventually breaks the nanowire [7]. A free, unsuspended chain of atoms would be totally unstable against an even larger set of deformations, for the final stable configuration will be a cluster, approximately spherical in shape, with a surface dominated by close-packed facets.

In our calculations, we address strictly the straight wire geometry, with equidistant atoms. One could imagine more complicated monostrand wire geometries, for example zigzag geometries [8] or Peierls distortions, leading to di- tri- or multimerization [9]. Such distorted configurations of an unsuspended monostrand wire may represent interesting local minima or saddle points in the total energy. When suspended between leads, however, local minima or saddle points of the string tension are to be considered instead of those of the energy, since they alone will correspond to long-lived, or 'magic' nanowires [7]. In Au, the zigzag deformations do not survive the string tension, and the same would happen, if they existed, in Ru, Rh, and Pd. Thus, we shall ignore zigzag distortions, since they are soft against tension, in the systems we address here. Peierls di-, tri- or multimerization distortions are critically dependent on a long wire as well as on a precise Fermi surface nesting, and would lead to insulating nanowires. In Ru, Rh, and Pd, the reported nanocontacts are three atoms long at most [4]. Moreover, there is no unique nesting since multiple bands cross the Fermi level, the precise Fermi crossings are tension-dependent, and the corresponding incommensurate order parameters are likely suppressed by size. The experimental evidence that nanocontacts of Ru, Rh, and Pd are consistently metallic further suggests neglecting Peierls distortions too until there is evidence to the contrary.

In wires, the electrons are confined in two dimensions. Before investigating in more detail what effect that has on the magnetic properties of Ru, Rh, and Pd, let us summarize briefly what is known about the magnetic properties of these metals when the electrons are confined only in one dimension, or in all three.

In a monolayer grown on, or sandwiched between, magnetically 'inert' substrates such as Cu, Ag, Au, or graphite, the electrons are at least approximately confined in one dimension, opening up the possibility for two-dimensional magnetism. The search for two-dimensional magnetism in Ru, Rh or Pd in such systems has been conducted extensively both theoretically and experimentally. Starting with Ru, a monolayer of this metal has been observed to order ferromagnetically when grown on graphite [10], and when layered between graphene

[5] In the case of Pd, we also performed antiferromagnetic calculations, but found this magnetic configuration to be unstable with respect to ferromagnetic ordering.

sheets [11]. No magnetism has been observed for Ru monolayers grown on Ag or Au surfaces. Theoretical calculations predict a Ru monolayer to be magnetic on graphite (under certain conditions) [12, 13], Ag [14, 15] and Au [15], but nonmagnetic on Cu [16]. For Rh metal, the only case in which two-dimensional magnetism has been observed is in a superlattice structure of Rh monolayers sandwiched between adjacent graphene sheets [11]. Monolayers of Rh grown on Ag, Au, or graphite have not shown any signs of magnetic order [17–19]. In great contrast to the experimental results, Rh monolayers have been predicted to order ferromagnetically on Cu [16], Ag [14, 15], Au [20, 15], and graphite [12, 13]. Finally, it has been predicted that a monolayer of Pd should be nonmagnetic on all substrates tested (Cu [16], Ag [14, 21, 22], and graphite [12, 13]). However, for Pd (and also Rh) films on Ag, calculations predict that the magnetic moment of the film is periodically suppressed and enhanced due to quantum well effects as a function of film thickness, giving rise to a finite ferromagnetic moment in certain films thicker than one monolayer [22].

All in all, the discrepancy between theory and experiment regarding magnetism in Ru and Rh monolayers appears to be rather large at present. One possible explanation for this discrepancy is diffusion of transition-metal atoms into the substrate, at least when the substrate is a noble metal. For Rh on graphite, the intricacies of this system have been discussed in detail in [19].

If we reduce the scale of all three dimensions down to nanometre size, we end up with clusters. Small Ru, Rh, and Pd clusters have been predicted to have magnetic ground states [23–26]. Experimentally, magnetism has been observed in Rh and Pd clusters. Counter-intuitively, large Pd clusters appear to be magnetic whereas small Pd clusters are not [27–29].

Returning to magnetism in nanowires, it has been predicted that monatomic rows of Rh on Ag(001) are ferromagnetic, using a semi-empirical tight-binding method [30]. Monatomic rows of Ru, Rh, and Pd on vicinal surfaces of Ag have also been studied theoretically using a screened Korringa–Kohn–Rostocker Green function method [31], predicting magnetism to appear in Ru and Rh chains, but not in Pd chains. Further, Spišák and Hafner [32] predict ferromagnetism in Ru and Rh rows grown on the Ag(117) vicinal surface, using the projector augmented plane-wave computational method. Similarly, they also find a ferromagnetic ground state for Ru rows grown on Cu(117), and for freely hanging Ru and Rh monostrand nanowires.

Regarding the objects we study in this paper, i.e., monostrand wires hanging between leads, we can actually get some first clues about possible magnetism simply by starting from the atomic ground state of Ru, Rh, Pd, and Ag and analysing the effect of a very weak hybridization of orbitals on adjacent atoms. In wire form, Ru and Rh could conceivably develop Hund's rule magnetism, due to their partially empty narrow bandwidth d shell. The Pd atom has in fact a filled 4d shell, but sd hybridization in the wire enables d $\rightarrow$ s electron transfer, opening up the possibility to spin-polarize Pd d-holes. Ag, on the other hand, is basically an sp metal, with the 4d shell completely filled in all cases. Interestingly, it is in principle possible that wires of metals like Ag (a typical system that might be thought of as a jellium) in themselves magnetize under certain conditions, since even a jellium confined in a thin cylinder in principle magnetizes for certain radii of the cylinder [33]. However, the moment formation in that case is weak and confined to very special radii or electron densities, and the associated energy gain is very small. That is of course so because exchange interactions, as described by Hund's first rule, are not particularly strong in an sp band metal or jellium. The situation is radically different for transition metals. Because of the partly occupied d-orbitals, their ability to magnetize is much stronger and of a fundamentally different nature compared to the jellium.

In the discussion above we have completely neglected the issue of fluctuations. Thermal fluctuations in a nanowire are expected to be very large, and would destroy long range magnetic order in the absence of an external magnetic field. In earlier papers [34, 35], we have argued in

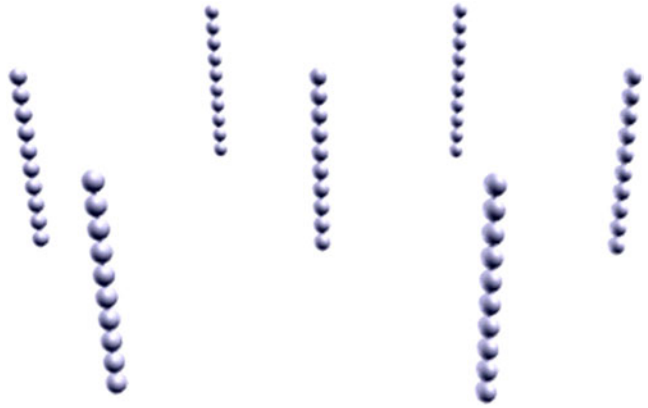

Figure 1. Sketch [43] of the setup. Infinitely long wires extend along the z-direction and form a hexagonal mesh in the xy-plane.

more detail how one might deal with fluctuations, and in what cases one can approximate some properties of the superparamagnetic state with those of a statically magnetized one (which is what we calculate), and we will not repeat those arguments here. Experimentally, evidence of one-dimensional superparamagnetism with fluctuations sufficiently slow on the timescale of the probe has been recently reported for Co atomic chains deposited on Pt surface steps [36].

2. Method

The technical aspects of the present calculations are similar to those reported in our earlier papers on 5d metal nanowires [34]. For the present density-functional-based [37] electronic-structure calculations we used the all-electron full-potential linear muffin-tin orbital method (FP-LMTO) [38]. This method assumes no shape approximation of the potential or wavefunctions. The calculations were performed using the generalized gradient approximation (GGA) [39]. As a test, some calculations were also performed using the local density approximation (LDA) [40], giving results very similar to the GGA ones. Further, some calculations were double-checked using the WIEN code [41, 42], again with very similar results.

The calculations were performed with inherently three-dimensional codes, and thus the system simulated was an infinite two-dimensional array of infinitely long, straight wires. Figure 1 shows a sketch of the setup. A one-dimensional Brillouin zone was used, i.e. the k-points form a single line, stretching along the z-axis of the wire. The Bravais lattice in the xy-plane was chosen hexagonal. With this choice, the d_{xy} and $d_{x^2-y^2}$ orbitals become automatically degenerate, as they should for a single wire. Furthermore, we used non-overlapping muffin-tin spheres with a constant radius in the calculations of the equilibrium bond lengths d. The magnetic moments, bands structures, conductance-channel curves and band widths were calculated using muffin-tin spheres scaling with the bond length. Convergence of the magnetic moment was ensured with respect to k-point mesh density, Fourier mesh density, tail energies, and wire–wire vacuum distance.

We performed both scalar relativistic (SR) calculations, and calculations including the spin–orbit coupling as well as the scalar relativistic terms. The latter will be referred to as 'fully relativistic' (FR) calculations in the following, although we are not strictly solving the

Table 1. Calculated bulk and wire equilibrium bond length d. Also shown are the wire magnetic moments per atom, calculated at the equilibrium bond length. The right-most column displays the experimental ground-state configuration for the free atoms. (FR = fully relativistic calculation; SR = scalar relativistic calculation).

Metal	Wire d (Å) FR	Bulk d (Å) FR	Bulk d (Å) exp.	Moment (μ_B) FR; SR	Free atom configuration
Ru	2.27	2.70	2.71	1.1	4 ($^5F_5$)
Rh	2.31	2.72	2.69	0.3	3 ($^4F_{9/2}$)
Pd	2.56	2.78	2.75	0.7	0 ($^1S_0$)
Ag	2.68	2.93	2.89	—	1 ($^2S_{1/2}$)

full Dirac equation, or making use of current density functional theory. In the fully relativistic calculations, the spin axis was chosen to be aligned along the wire direction.

3. Results

3.1. Bond lengths and energetics

In a monostrand nanowire, there are only two nearest neighbours, and therefore we expect the bond length minimizing the total energy to be smaller than in the bulk. This is indeed the case, as can be seen in table 1, where calculated bond lengths for monowires and bulk are listed, together with the experimental bulk values. Our bulk GGA calculations for the equilibrium bond lengths are in very close agreement with the experimental values. Our calculated bond lengths for free-standing, monostrand wires are close to (within a few hundredths of an ångström) the ones reported in [44] (Pd and Ag), but significantly larger than (the differences are of the order 0.1 Å) the ones reported in [32] (Ru, Rh, and Pd). We also wish to point out here that, strictly speaking, a tip-suspended wire will not have a quasi-stable configuration at the bond length which minimizes the total energy, but at a slightly larger value since it is rather the string tension than the total energy which should attain a local minimum [7]. Nevertheless, for simplicity, in the remainder of this paper, the bond length which minimizes the total energy will be called the equilibrium bond length.

Table 1 also shows our calculated mean-field magnetic moments per atom at the equilibrium bond lengths. Note that the scalar relativistic and fully relativistic calculations predict the same magnetic moments within the precision given at the equilibrium bond length. Thus, the spin–orbit coupling appears to be unimportant in regard to the existence and magnitude of the magnetic moments in the 4d metals Ru, Rh, and Pd. This makes a strong contrast to the situation in 5d nanowires of Os, Ir, and Pt, where relativistic effects were shown to be crucial for the correct description of the magnetic profiles [34]. Even for the 4d metal nanowires, however, it turns out that the spin–orbit coupling is by no means unimportant, as will be further elucidated in the analysis of the energetics, band structures, and conductance channels. Calculated magnetic moments for straight monostrand wires of Ru and Rh have also been reported by Spišák and Hafner [32]. They found 0.98 μ_B for Ru, and 0.26 μ_B for Rh, which is in excellent agreement with our calculated spin moments. Our result for Pd differs from that of Bahn *et al* [44] who found no magnetism in pseudopotential calculations for Pd monostrand nanowires. It seems possible that the disagreement could arise in this very borderline case due to the different methods used, in which case we would tend to trust our all-electron approach better. Experiments will have to be awaited in order to settle this question.

Table 2. Total energy difference between wire and bulk, and between the nonmagnetic and ferromagnetic wire, per atom. (SR = scalar relativistic calculation; FR = fully relativistic calculation; NM = nonmagnetic calculation; FM = ferromagnetic calculation).

Metal	$E_{\mathrm{wire}}-E_{\mathrm{bulk}}$ (eV) SR	$E_{\mathrm{wire}}-E_{\mathrm{bulk}}$ (eV) FR	$E_{\mathrm{NM}}-E_{\mathrm{FM}}$ (meV) SR	$E_{\mathrm{NM}}-E_{\mathrm{FM}}$ (meV) FR
Ru	5.4	4.9	77	56
Rh	4.7	4.1	10	9
Pd	3.1	3.1	25	12
Ag	1.8	1.8	—	—

The right-most column in table 1 lists the experimental atomic ground state configuration, showing that the free Ru, Rh, Pd, and Ag atoms have spin moments of 4, 3, 0, and 1 μ_{B}, respectively. Thus, we see that the predicted wire moments at the equilibrium bond length are much smaller than the magnetic moments of the free atom, except for Pd, where the atomic moment is zero, but the wire has a substantial magnetic moment of around 0.7 μ_{B}.

In order to analyse the relative stability of wire formation, we calculated the energy difference between wire and bulk. The results are displayed in table 2. The energy difference between wire and bulk is smallest for Ag (1.8 eV), and increases as one goes left in the 4d series to Pd, Rh and Ru. Spin–orbit coupling somewhat reduces this energy difference by about 0.5 eV for Ru and Rh, whereas it has no effect in Pd and Ag. Scalar relativistic energy differences between monowire and bulk have been reported earlier for Pd and Ag, and our numbers agree well with that calculation [44].

We also calculated the energy gain when the wire is allowed to spin-polarize, $E_{\mathrm{NM}}-E_{\mathrm{FM}}$. This quantity is typically a few hundredths of an electronvolt, and differs greatly from element to element. Spin–orbit coupling halves $E_{\mathrm{NM}}-E_{\mathrm{FM}}$ in the case of Pd, whereas the effect of spin–orbit coupling on magnetism is much smaller for Rh and Rh. In [32], this energy difference was reported to be 39 meV for Ru, and 6 meV for Rh, i.e., smaller compared to the ones calculated in the present work (56 and 9 meV, respectively).

3.2. Magnetic moments and band structures

The magnetic moments per atom as a function of nanowire bond length are shown in the left-most column of figure 2. The solid lines refer to the fully relativistic calculations (magnetization parallel to the wire), and the dotted lines to the scalar relativistic calculations. All the metals studied, except Ag, exhibit a magnetic moment for values of the bond lengths at equilibrium. Spin–orbit coupling apparently has a very limited effect on the magnetic profiles; for Ru and Rh, the difference is not even visible; for Pd, however, there is a small but visible quantitative difference.

The magnetic profiles for Ru and Rh are quite similar to each other. For both metals, the magnetic moment increases with stretching, and reaches a plateau value for large bond lengths. The magnetic profile of Pd, on the other hand, is unique in that it has a maximum for bond lengths around the equilibrium value, and then decreases down to zero for stretched bond lengths (see also [35] for a more in-depth discussion of the Pd nanowire magnetic profile). The Ag wire is, unsurprisingly, firmly nonmagnetic for the bond lengths studied.

In order to shed some light onto the mechanisms behind the magnetic profiles displayed in figure 2, we will now analyse the electronic structure of the wires with the help of the band structures at different bond lengths.

Band structures for two different bond lengths, the equilibrium bond length, and a larger one of 2.9 Å, roughly representing two magnetic regimes, are shown in figure 3 (fully relativistic

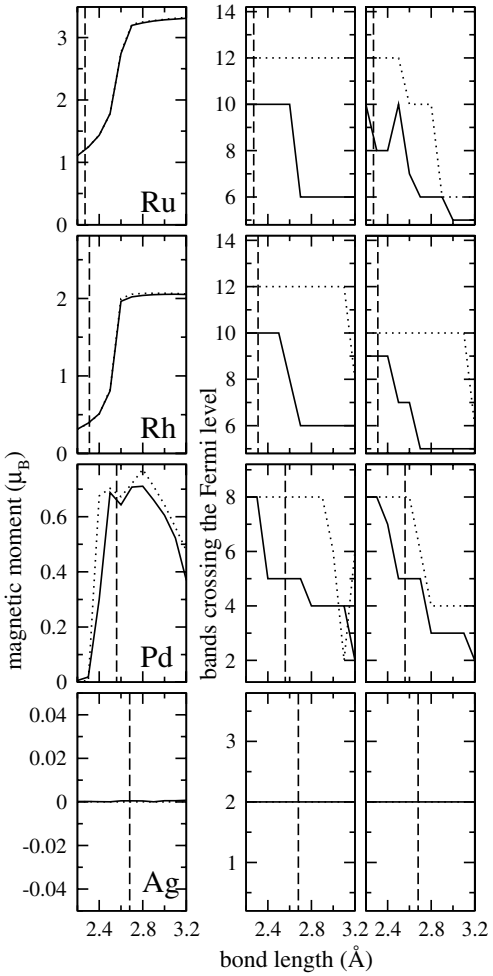

Figure 2. Magnetic profiles and number of bands crossing the Fermi level for the four metals studied. The left-most column shows total magnetic moments per atom, as a function of bond length, both with spin–orbit coupling (FR, solid line) and without (SR, dotted line). The middle and right-most columns show the number of bands crossing the Fermi level as a function of bond length for the SR and FR calculation, respectively. The solid lines refer to ferromagnetic calculations, and the dotted lines are for nonmagnetic calculations. The dashed vertical lines point out the equilibrium bond lengths.

calculation) and figure 4 (scalar relativistic calculation) for each of the four metals studied. The bands run from the zone centre, Γ, to the zone edge, A, in the direction of the wire.

The character of the bands close to the Fermi level is of critical importance for the moment formation, and therefore we also show character-resolved bands; see figure 5. We found it useful to split up the d character into three contributions: d_z, (d_{xz}, d_{yz}) and (d_{xy}, $d_{x^2-y^2}$). Thus, figure 5 has four panels, displaying separately the s, d_z, (d_{xz}, d_{yz}) and (d_{xy}, $d_{x^2-y^2}$) characters of the bands. The vertical error bars, or 'thickness', of the bands indicate the relative character weight. The data in figure 5 have been taken from a scalar relativistic calculation for Pd. For the other metals, the relative weights of the orbitals for each band are qualitatively similar to the ones shown. From figure 5, we see that most bands in the vicinity of the Fermi level are

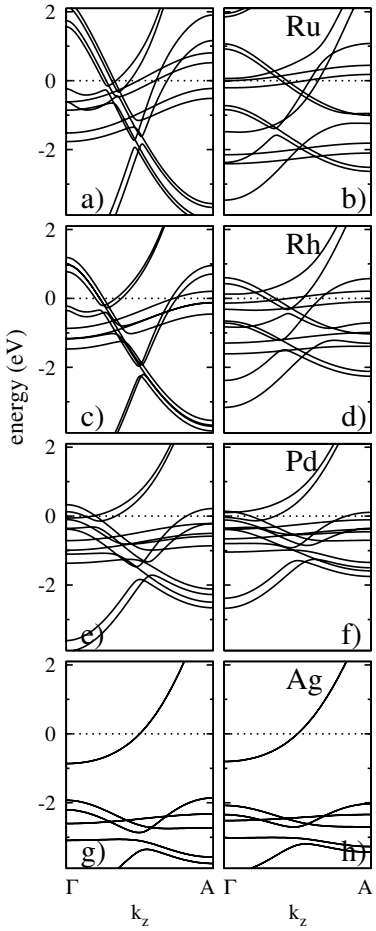

Figure 3. FR band structures, along the wire direction, at two different bond lengths (the equilibrium one, and a larger of 2.9 Å) for each element. The Fermi energy is at zero. Band doubling (present in panels (a) through (f)) indicates spin splitting due to magnetic order.

of predominantly d character. In fact, there are only two bands with some s character crossing the Fermi level (see upper left panel in figure 5). Of these, the highest lying band crosses the Fermi level closer to the zone centre than the zone edge, at about one third of the distance between the zone centre and zone edge. The second one of the two s-containing bands crosses the Fermi level very close to the zone edge (A). At that point, this band has some s character, but is in fact dominated by d_z character.

At Γ and A (both critical points by symmetry), all band dispersions are horizontal. This gives rise to very sharp $1/\sqrt{E}$ band edge van Hove singularities, due to the one-dimensionality of the systems. If a band has mostly d character at the edge, the exchange energy gain will be rather large if the band spin-splits so that one of the spin-channel band edges ends up above the Fermi level, and the other one below. We note in passing that, strictly speaking, in the fully relativistic calculations (figure 3) the spin–orbit coupling will mix the two spin channels so that, in general, an eigenvalue will have both majority and minority spin character. However, in the present calculations, this mixing is so small, typically just a few per cent, that it is irrelevant for our qualitative discussion here. Thus, if a band edge ends up sufficiently near

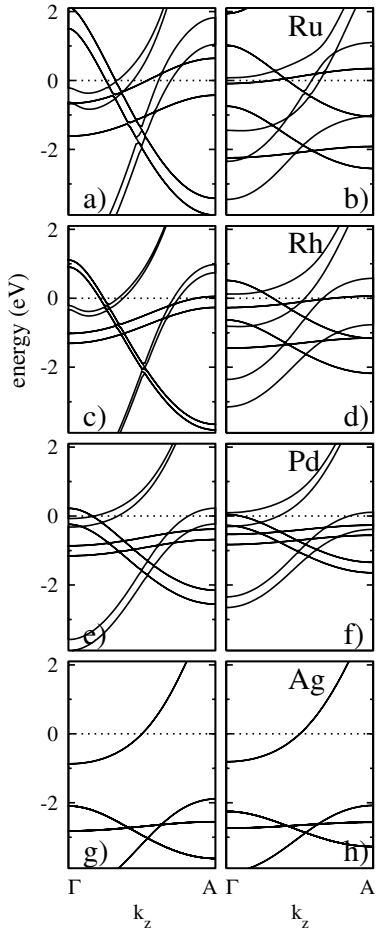

Figure 4. SR band structures, along the wire direction, at two different bond lengths (the equilibrium one, and a larger of 2.9 Å) for each element. The Fermi energy is at zero. Band doubling (present in panels (a) through (f)) indicates spin splitting due to magnetic order.

the Fermi level, we may expect a magnetic moment to develop. While apparently similar to the magnetization of the jellium wire [33], the magnetism here is much more substantial, since here the d-states involve a much stronger Hund's rule exchange. We now go through all four metals, starting with Ru, analysing how the band edges move as a function of bond length, and how this affects the magnetic state of the wires.

Ru. The magnetic moment of Ru increases with the bond length. At the equilibrium bond length, the rather flat (d_{xy}, $d_{x^2-y^2}$) bands are split around the Fermi level, creating a relatively large magnetic moment of 1.1 μ_B, see panel (a) in figures 3 and 4. The (d_{xz}, d_{yz}) bands are still broad at this bond length and in principle unpolarized. As the bond length increases, the (d_{xz}, d_{yz}) bands narrow down and eventually also spin-polarize. They split around the Fermi level, and causes a large magnetic moment of more than 3 μ_B for bond lengths larger than 2.7 Å.

Rh. As in Ru, the magnetic moment of Rh increases with the bond length. In fact, the magnetic profile for Rh is very similar to the one of Ru, just shifted in magnitude. With one

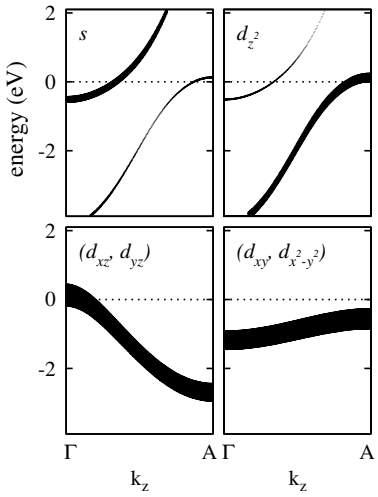

Figure 5. Character-resolved SR band structure for non-spin-polarized Pd, along the wire direction. The Fermi energy is at zero. The d_{xz} and d_{yz} orbitals are always degenerate, and the same is true for the orbital pair d_{xy} and $d_{x^2-y^2}$.

more electron than Ru, the bands of the Rh wire lie generally deeper. The result is that the flat (d_{xy}, $d_{x^2-y^2}$) bands barely touch the Fermi level, instead of clearly crossing it, as in Ru. The result is a smaller splitting, and consequently a smaller moment. With increasing bond length, all the other bands also narrow down and eventually split around the Fermi level, just like for Ru. The result is a plateau value of the magnetic moment of about 2 μ_B for bond lengths above 2.6 Å. Thus, in both Ru and Rh, the flat (d_{xy}, $d_{x^2-y^2}$) bands drive the formation of the magnetic moment, and the (d_{xz}, d_{yz}) bands enhance it.

Pd. In Pd, the very same flat (d_{xy}, $d_{x^2-y^2}$) bands leading to Hund's rule magnetism in Ru and Rh are entirely occupied at all bond lengths studied. The spin-polarization is instead driven by the s + d_{z^2} and (d_{xz}, d_{yz}) bands, which have a high dispersion, and display one-dimensional band edges close to the Fermi level at Γ and A. In the magnetic regime, it happens that these three band edges all are nearly degenerate in energy and close to the Fermi level. This accidental feature of the long Pd monostrand nanowire band structure dramatically increases the density of states, since divergent van Hove singularities are formed close to the Fermi level. For the stretched wire with bond length 2.9 Å (panel (f) in figures 3 and 4), the s-dominated band with band edge at Γ is split around the Fermi level. A more detailed discussion of the physics of Pd nanowires can be found in [35].

Ag. For Ag, basically an sp metal, all the d-bands are filled and there is never any d-magnetism. The only band crossing the Fermi level is one of the s-dominated, high-dispersion, s + d_{z^2} bands. Calculations have shown that monostrand wires of sp metals, and even a jellium cylinder, can spin-split [33, 45]. For this to happen, however, a band edge must be extremely close to the Fermi level. The s + d_{z^2} band in the Ag wire has a band edge at Γ approximately 1 eV below the Fermi level, which is too far down to make a spin splitting possible.

3.3. Ballistic conductance channels

As seen from the above discussion of the nanowire band structures, spin splitting of bands does alter n, i.e., the number of bands (or channels) crossing the Fermi level. By virtue of the

Landauer formula

$$G = \frac{e^2}{h} \sum_i \tau_i, \tag{1}$$

where τ_i is the transmission through channel i, the maximum theoretical ballistic conductance has, in units of $\frac{1}{2}G_0 = e^2/h$, precisely the number of bands n crossing the Fermi level as its upper limit. Thus, the conductance through the wires should be affected by the presence of magnetism.

The middle column of figure 2 (fully relativistic calculation) and right-most column of figure 2 (scalar relativistic calculation) illustrate how n is influenced by nanowire spin-polarization, bond length, and spin–orbit coupling. For Ru, Rh, and Pd in their magnetized state at the equilibrium bond length, n is 9, 9, and 5, respectively, compared to 12, 10, and 8 in the nonmagnetic state when spin–orbit coupling is included in the calculation. In the scalar relativistic calculations, the channel count at the equilibrium bond length for Ru and Rh is close to but not identical to the channel count of the fully relativistic calculation. For Pd the two calculations give the same channel count at equilibrium bond length. For stretched wires, however, the scalar and fully relativistic calculations differ also for Pd in the number of conductance channels.

In general, spin-polarization tends to decrease the number of channels. Should all the channels transmit fully, large ballistic conductances of $4.5G_0$, $4.5G_0$, and $2.5G_0$ for Ru, Rh, and Pd, respectively would ensue, to be compared with nonmagnetic conductances of $6G_0$, $5G_0$, and $4G_0$, respectively.

In reality, however, the situation will be quite different, due to the fact that most of the open channels have d character. While the conductance of the s-dominated channels is generally close to one owing to nearly complete transmission, that of the d-channels is much smaller, with a high reflection at the lead-wire junction, generally dependent on the detailed junction geometry. Our calculations reveal that the occupation of each of the two s-channels is always finite for all bond lengths reported here, bringing an expected contribution close to G_0 to the total conductance. The d-channel contribution to the conductance is expected to be much smaller than $\frac{1}{2}G_0$ per channel. All in all, we may thus expect monatomic nanocontacts of Ru, Rh, and Pd to have a conductance above G_0 but well below $4.5G_0$, $4.5G_0$, and $2.5G_0$, respectively. Since the scattering of the d-waves at the junctions depends highly on the geometry, whose details will change at every realization, we also expect the conductance histograms to exhibit peaks that could be both broad and poorly reproducible.

Conductance histograms and traces for Ru and Rh nanocontacts have been measured by Itakura *et al* [3]. In both these metals, they find a broad bump between G_0 and $2G_0$, which is consistent with our results.

Enomoto *et al* [46] have published conductance histograms and traces for Pd–Ag alloys. In their conductance histogram for pure Pd, there is no significant structure in the region G_0–$4G_0$, whereas for Ag, there is a sharp peak at G_0, as expected. Rodrigues *et al* [4] have measured the conductance through pure Pd nanocontacts in ultra-high vacuum, and found a peak at very low conductance, around $0.5G_0$.

4. Discussion and conclusions

Our all-electron calculations suggest that the Ru, Rh, and Pd monatomic nanowires exhibit spontaneous Hund's rule magnetism for values of the bond length at and around equilibrium. The energy gain connected with the magnetic state is of the order of a few hundredths of an electronvolt. This indicates that the magnetization could be stabilized against fluctuations at

cryogenic temperatures, especially with the help of an external field. From a methodological point of view, the spin–orbit coupling is found to be important for a correct description of the energetics, and the number of d-dominated conductance channels. In contrast, the spin moments themselves are rather insensitive to the spin–orbit coupling.

How might this nanomagnetism be detected experimentally? Merely measuring the conduction through the wire at one single temperature and magnetic field strength will most probably not give conclusive information regarding the magnetic state of the atoms in the wire, since the transmission through d-channels is rather poor, varies greatly with geometry and can hardy be regarded as quantized. We speculate that the conductance may vary in the following qualitative way as a function of temperature and magnetic field strength. First, at low temperature and zero field a Kondo state between the conduction electrons and the nanomagnet could form, implying a high ballistic conductance [48]. Second, at high temperature and zero field Kondo-like effects could affect the ballistic conductance and cause it to drop [48]. Third, low temperature and a high magnetic field would take the nanowire to a magnetic, or in any case to a slowly fluctuating superparamagnetic, regime. In this regime the number of conductance channels should diminish, and so should the conductance. At sufficiently low temperatures, the conductance should therefore be field sensitive, and that magnetoresistance would be a clear indication of a magnetic state. Therefore, a key experiment would be to measure ballistic conductance as a function of both temperature and external magnetic field.

Fractional conductance peaks below G_0 have been observed experimentally, for example the $\frac{1}{2}G_0$ peak reported by Ono for Ni [47], and very recently by Rodrigues *et al* for Co, Pd and Pt [4], at room temperature and zero field. These results are intriguing, since we expect that the s-channels alone should yield a conductance larger than that. Impurities could be a possible explanation for these low-conductance peaks, as Untiedt *et al* [49] very recently demonstrated in the case of Pt. But several questions remain, such as why the $\frac{1}{2}G_0$ peak is much larger in Co and Pd than in Pt [4]. Therefore, it would be highly interesting to see if the half-conductance peak exists also in conductance histograms of Ru and Rh, and how the relative size of that peak, if it exists, varies with impurity concentration. We discussed in previous work [50] a possibility to obtain conductance G_0 from a magnetic transition metal nanowire with a magnetization reversal occurring inside the nanowire. This could in principle drop to $\frac{1}{2}G_0$ in an asymmetrical situation, with a net prevalence of majority spins over minority spins. We are however at the present time not able to explain how that kind of state could be sustained in Pd, at the experimental conditions of zero field and room temperature. Finally, we also note that the conductance histogram peaks in [4] for Co, Pd, and Pt, centred around $\frac{1}{2}G_0$, are rather broad, which suggests that they might not be caused by one single fully transmitting spin-polarized channel, but perhaps by several poorly conducting channels. In any case, more theory work will be needed to address the experimental data, explicitly including such elements as tip form, spin structures, impurities [49], strong correlations, and temperature as well as their effects on the system's conductance.

Acknowledgments

AD acknowledges financial support from the European Commission through contract no. HPMF-CT-2000-00827, STINT (Swedish Foundation for International Cooperation in Research and Higher Education), and VR (Swedish Research Council). Work at SISSA was also sponsored through TMR FULPROP, MIUR (COFIN and FIRB) and by INFM/F. Ruben Weht is acknowledged for discussions, and for double-checking some of the calculations using the WIEN97 code. J M Wills is acknowledged for letting us use his FP-LMTO code. We are

also grateful to D Ugarte for sharing with us the results of [4] prior to publication, and to C Untiedt for several discussion.

References

[1] Kondo K and Takayanagi K 2000 *Science* **289** 606
[2] Rodrigues V, Fuhrer T and Ugarte D 2000 *Phys. Rev. Lett.* **85** 4124
[3] Itakura K, Yasuda H, Kurokawa S and Sakai A 2000 *J. Phys. Soc. Japan* **69** 625
[4] Rodrigues V, Bettini J, Silva P C and Ugarte D 2003 *Phys. Rev. Lett.* **91** 096801
[5] van Wees B J, van Houten H, Beenakker C W J, Williamson J G, Kouwenhoven L P, van der Marel D and Foxon C T 1988 *Phys. Rev. Lett.* **60** 848
[6] Gülseren O, Ercolessi F and Tosatti E 1998 *Phys. Rev. Lett.* **80** 3775
[7] Tosatti E, Prestipino S, Kostlmeier S, Dal Corso A and Di Tolla F D 2001 *Science* **291** 288
[8] Sanchez-Portal D, Artacho E, Junquera J, Ordejón P, García A and Soler J M 1999 *Phys. Rev. Lett.* **83** 3884
[9] Peierls R E 1955 *Quantum Theory of Solids* (London: Oxford University Press)
[10] Pfandzelter R, Steierl G and Rau C 1995 *Phys. Rev. Lett.* **74** 3467
[11] Suzuki M, Suzuki I S and Walter J 2003 *Phys. Rev.* B **67** 094406
[12] Chen L, Wu R, Kioussis N and Blanco R J 1997 *J. Appl. Phys.* **81** 4161
[13] Krüger P, Parlebas J C, Moraitis G and Demangeat C 1998 *Comput. Mater. Sci.* **10** 265
[14] Eriksson O, Albers R C and Boring A M 1991 *Phys. Rev. Lett.* **66** 1350
[15] Blügel S 1992 *Europhys. Lett.* **18** 257
[16] García A E, González-Robles V and Baquero R 1999 *Phys. Rev.* B **59** 9392
[17] Beckmann H and Bergmann G 1997 *Phys. Rev.* B **55** 14350
[18] Chado I, Scheurer F and Bucher J P 2001 *Phys. Rev.* B **64** 094410
[19] Goldoni A, Baraldi A, Comelli G, Esch F, Larciprete R, Lizzit S and Paolucci G 2001 *Phys. Rev.* B **63** 035405
[20] Zhu M J, Bylander D M and Kleinman L 1991 *Phys. Rev.* B **43** 4007
[21] Redinger J, Blügel S and Podloucky R 1995 *Phys. Rev.* B **51** 13852
[22] Niklasson A M N, Mirbt S, Skriver H L and Johansson B 1997 *Phys. Rev.* B **56** 3276
[23] Galicia R 1993 *R. Mex. Fis.* **32** 51
[24] Reddy B V, Khanna S N and Dunlap B I 1993 *Phys. Rev. Lett.* **70** 3323
[25] Vitos L, Johansson B and Kollar J 2000 *Phys. Rev.* B **62** 11957
[26] Moseler M, Häkkinen H, Barnett R N and Landman U 2001 *Phys. Rev. Lett.* **86** 2545
[27] Cox A J, Louderback J G, Apsel S E and Bloomfield L A 1994 *Phys. Rev.* B **49** 12295
[28] Sampedro B, Crespo P, Hernando A, Litrán R, Sánchez López J C, López Cartes C, Fernandez A, Ramírez J, González Calbet J and Vallet M 2003 *Phys. Rev. Lett.* **91** 237203
[29] Taniyama T, Ohta E and Sato T 1997 *Europhys. Lett.* **38** 195
[30] Bazhanov D I, Hergert W, Stepanyuk V S, Katsnelson A A, Rennert P, Kokko K and Demangeat C 2000 *Phys. Rev.* B **62** 6415
[31] Bellini V, Papanikolaou N, Zeller R and Dederichs P H 2001 *Phys. Rev.* B **64** 094403
[32] Spišák D and Hafner J 2003 *Comput. Mater. Sci.* **27** 138
Spišák D and Hafner J 2003 *Phys. Rev.* B **67** 214416
[33] Zabala N, Puska M J and Nieminen R M 1998 *Phys. Rev. Lett.* **80** 3336(C)
Zabala N, Puska M J and Nieminen R M 1999 *Phys. Rev. Lett.* **82** 3000(R)
[34] Delin A and Tosatti E 2003 *Phys. Rev.* B **68** 144434
Delin A and Tosatti E 2004 *Surf. Sci.* **566–568** 262
[35] Delin A, Tosatti E and Weht R 2004 *Phys. Rev. Lett.* **92** 057201
[36] Gambardella P, Dallmeyer A, Maiti K, Malagoli M C, Eberhardt W, Kern K and Carbone C 2002 *Nature* **416** 301
[37] Hohenberg P and Kohn W 1964 *Phys. Rev.* **136** B864
Kohn W and Sham L J 1965 *Phys. Rev.* **140** A1133
[38] Wills J M, Eriksson O, Alouani M and Price O L 2000 *Electronic Structure and Physical Properties of Solids* ed H Dreyssé (Berlin: Springer)
[39] Perdew J P, Burke K and Ernzerhof M 1996 *Phys. Rev. Lett.* **77** 3865
Perdew J P, Burke K and Ernzerhof M 1997 *Phys. Rev. Lett.* **78** 1396
Zhang Y and Yang W 1998 *Phys. Rev. Lett.* **80** 890
Perdew J P, Burke K and Ernzerhof M 1998 *Phys. Rev. Lett.* **80** 891
[40] Ceperley D M and Alder B J 1980 *Phys. Rev. Lett.* **45** 566
Perdew J P and Zunger A 1981 *Phys. Rev.* B **23** 5048

[41] Singh D J 1994 *Planewaves, Pseudopotentials, and the LAPW Method* (Boston, MA: Kluwer–Academic)
[42] Blaha P, Schwarz K and Luitz J 1997 *Computer code WIEN97* Vienna University of Technology, Vienna
Improved and updated UNIX version of the original copyrighted WIEN code, which was published by Blaha P, Schwarz K, Sorantin P and Trickey S B 1990 *Comput. Phys. Commun.* **59** 339
[43] This figure was produced using the XCrySDen package available from http://www.xcrysden.org/
Kokalj T 1999 *J. Mol. Graphics Modelling* **17** 176
[44] Bahn S R and Jacobsen K W 2001 *Phys. Rev. Lett.* **87** 266101
[45] Ayuela A, Raebiger H, Puska M J and Nieminen R M 2002 *Phys. Rev.* B **66** 035417
[46] Enomoto A, Kurokawa S and Sakai A 2002 *Phys. Rev.* B **65** 125410
[47] Ono T, Ooka Y, Miyajima H and Otani Y 1999 *Appl. Phys. Lett.* **75** 1622
[48] See, e.g., Costi T A 2000 *Phys. Rev. Lett.* **85** 1504
[49] Untiedt C, Dekker D M T, Djukic D and van Ruitenbeek J M 2004 *Phys. Rev.* B **69** 081401
[50] Smogunov A, Dal Corso A and Tosatti E 2002 *Surf. Sci.* **507** 609